

## Response to Reviewer 1 Comments

We truly grateful for the reviewers for the valuable and constructive comments, which are very useful for the improvement of the manuscript. We have revised the manuscript carefully according to the reviewers' comments. Point-to-point responses are given below. The original comments are black in color, while our responses are in blue. The revised parts in the manuscript are marked in red. All the page number and line number are referred to the revised manuscript.

### General comments:

**Point 1:** It's hard for me to identify the main topic of this paper. While the primary focus appears to be explaining the opposing trends in the 98<sup>th</sup> and 2<sup>nd</sup> percentiles of ozone in the MLYRP (part of eastern China), the paper includes many other analyses that are irrelevant to this topic. For instance, Section 3.4 (Interannual differences in surface O<sub>3</sub> formation sensitivity) and Section 3.6 (Key meteorological and anthropogenic factors inducing O<sub>3</sub> pollution) should be removed (they haven't found anything new in these sections either). The entire paper should be reframed. Additionally, Section 3.5 presents the same analysis and draws the same conclusions as Sections 3.1–3.3 but for a larger area (eastern China). The inclusion of Section 3.5 seems redundant. Why don't the authors focus on eastern China throughout the manuscript?

**Response 1:** We apologize for the confusion generated by the previous version of the manuscript and sincerely hope that our logic is now easier to follow with this new version. We have followed the reviewer's comments and reorganized the manuscript to avoid diverting the reader's attention. Firstly, we have deleted sections 3.4 (Interannual differences in surface O<sub>3</sub> formation sensitivity) and 3.6 (Key meteorological and anthropogenic factors inducing O<sub>3</sub> pollution) in the previous manuscript. Then, sections 3.1–3.3 and 3.5 was reframed, and the entire updated manuscript focuses on eastern China throughout the manuscript.

The new manuscript mainly includes four parts. First, we report long-term records of surface O<sub>3</sub> and related parameters observed at urban air quality monitoring sites and by satellites in eastern China, characterizing the trends of low, typical, and peak surface O<sub>3</sub> concentrations during the warm season (May–September) from 2017 to 2022. Then, a Multiple Linear Regression (MLR) model is used to evaluate the anthropogenic and meteorological contributions to the 98<sup>th</sup> and 2<sup>nd</sup> O<sub>3</sub> percentile trends. Next, secondary formaldehyde (HCHO) and NO<sub>2</sub> are employed to diagnose the diurnal variations in O<sub>3</sub> formation sensitivity and investigate the reasons for peak O<sub>3</sub> concentration trends in the context of current NO<sub>x</sub> reduction.

Finally, we discuss the reasons for the potential increase in low O<sub>3</sub> concentrations and the sensitivity of peak and low O<sub>3</sub> trends during the study period. Please refer to our new manuscript for details.

In addition, following the referee's suggestion, the manuscript was edited by Elsevier Language Editing Services (please see the following Elsevier certificate).



**Fig. R1** Certificate of Elsevier language editing services

**Point 2:** To understand the drivers of ozone trends, the authors use Multiple Linear Regression (MLR) to separate meteorological influences. There are several issues with their analysis: (a) The predicted variable, O<sub>3</sub> concentration, should also be normalized in the MLR. Normalizing Y first would eliminate the need for natural background O<sub>3</sub> in equation (2). (b) Line 27, Page 6, the statement that O<sub>3</sub> from natural sources is stable is incorrect. Biogenic VOCs and soil NO<sub>x</sub> emissions are highly sensitive to temperature. (c) Lines 19–21, 23–24, Page 10, the authors seem to confuse the terms “interannual fluctuation” and “trend.” The trend observed is actually a low–frequency signal after removing the high–frequency signals (interannual fluctuation). In this part, it is only acceptable to conclude that the anthropogenic component drives the trend, but it is apparent that meteorological parameters dominate the interannual fluctuation (as it roughly reproduces the peaks and troughs). All of this needs to be corrected.

**Response 2:** We thank the reviewer for pointing out this issue. (a) We corrected the problem (the predicted variable, O<sub>3</sub> concentration, should also be normalized in the MLR. Normalizing Y first would eliminate the need for natural background O<sub>3</sub> in equation 2) in the MLR model, and rearranged this subsection to conclude that, although anthropogenic emissions are the main driver of the opposing trends in peak and low O<sub>3</sub> concentrations in eastern China, the effect of

the change of meteorological component on 2<sup>nd</sup> or 98<sup>th</sup> O<sub>3</sub> percentiles trends cannot be ignored. (b) The statements in Line 27, Page 6 have been deleted, and (c) Lines 19–21, 23–24, Page 10 have been corrected.

In the new manuscript, we used the same stepwise MLR modeling approach as (Zhai et al., 2019; Li et al., 2018; Li et al., 2020; Liu et al., 2023). Following Liu et al. (2023) and Li et al. (2020), the MLR model fitted the deseasonalized and detrended 10 d mean 98<sup>th</sup> or 2<sup>nd</sup> O<sub>3</sub> percentile time series to the deseasonalized and detrended 10 d mean meteorological variables. The deseasonalized and detrended time series data were constructed by removing the 50 d moving average data from the 10 d moving average data. The stepwise MLR model has the following form:

$$Y(t) = R + \sum_{k=1}^n \beta_k X_k(t) \quad (1)$$

Where  $Y(t)$  is the deseasonalized and detrended daily surface 98<sup>th</sup> or 2<sup>nd</sup> O<sub>3</sub> percentile time series,  $R$  is the regression constant,  $\beta_k$  is the regression coefficient, and  $X_k$  is the deseasonalized and detrended daily meteorological variable considered as a possible O<sub>3</sub> covariate. Stepwise regressions were performed, adding and removing terms based on their independent statistical significance to obtain the best model fit.

Daily meteorological variables were obtained from the ERA5 reanalysis data (Download from <https://cds.climate.copernicus.eu>, last access: January 7, 2024), included temperature (T, °C), surface relative humidity (RH, %), total cloud cover (TCC), total precipitation (TP, mm), mean sea level pressure (MSLP, hPa), wind speed of U, V components (U, V, m/s), boundary layer height (BLH, m), and vertical velocity at 850 hPa (V850, m/s).

First, we used the MLR model to remove the effects of meteorological variability from the 2017 to 2022 98<sup>th</sup> or 2<sup>nd</sup> O<sub>3</sub> percentile trends. We apply Eq. (1) to the meteorological anomalies  $X_k$  during May–September 2017–2022, obtained by removing the 6–year means of the 50 d moving averages from the 10 d mean time series. The anomalies calculated in this process were deseasonalized but not detrended. This yields the meteorology–driven 98<sup>th</sup> or 2<sup>nd</sup> O<sub>3</sub> percentile anomalies  $Y_m(t)$

$$Y_m(t) = R + \sum_{k=1}^n \beta_k X_k(t) \quad (2)$$

Secondly, to avoid overfitting, only the three most important meteorological parameters were selected based on their individual contributions to the regressed 98<sup>th</sup> or 2<sup>nd</sup> O<sub>3</sub> percentiles, along with the requirement that they be statistically significant above the 95% confidence level

in the MLR model (Li et al., 2018). The fit results and selected meteorological variables varied by city but were regionally consistent (Table R1 and Table R2). The 98<sup>th</sup> or 2<sup>nd</sup> O<sub>3</sub> percentile anomalies  $Y_a(t)$  obtained by deseasonalizing, but not detrending, the 98<sup>th</sup> or 2<sup>nd</sup> O<sub>3</sub> percentile time series in a similar manner as for the meteorological variables (by removing the 6–year means of the 50 d moving averages). The residual anomaly  $Y_r(t)$  after removing the meteorology–driven 98<sup>th</sup> or 2<sup>nd</sup> O<sub>3</sub> percentile anomalies from the MLR model is given by

$$Y_r(t) = Y_a(t) - Y_m(t) \quad (3)$$

Finally, the residual is an anomalous component that cannot be explained by the MLR meteorological model and is referred to as meteorologically corrected data by (Zhai et al., 2019). It consists of noise due to the limitations of the MLR model and other factors and can be mainly attributed to long–term trends in anthropogenic emission changes over a 6–year period. The trend in the regressed 98<sup>th</sup> or 2<sup>nd</sup> O<sub>3</sub> percentile reflected the meteorological contribution, and the residual was then used to reflect the presumed anthropogenic contribution. For the updated MLR model, please refer to section 2.4 in the manuscript.

**Table R1.** Meteorological drivers of 2% O<sub>3</sub> percentile and Pearson correlation coefficient between observed and modeled 2% O<sub>3</sub> percentile in each city of eastern China during May–September 2017–2022

	Meteorological variable					Meteorological variable			
	1 <sup>st</sup>	2 <sup>st</sup>	3 <sup>st</sup>	R		1 <sup>st</sup>	2 <sup>st</sup>	3 <sup>st</sup>	R
Taian	T	RH	U	0.35	Beijing	U	RH	T	0.23
Puyang	T	BLH	RH	0.50	Tianjing	U	T	RH	0.32
Rizhao	U	V	T	0.46	Baoding	U	RH	TP	0.27
Jining	RH	T	V	0.54	Lanfang	U	T	V	0.23
Xinxiang	U	RH	V	0.41	Shijiazhuang	RH	BLH	U	0.27
Jiaozuo	T	RH	U	0.39	Handan	RH	V	BLH	0.20
Heze	RH	T	V	0.47	Qinghuangdao	V	U	RH	0.32
Linyi	RH	U	TP	0.40	Cangzhou	BLH	T	MSLP	0.28
Kaifeng	RH	U	T	0.49	Xingtai	RH	BLH	U	0.17
Zhengzhou	BLH	RH	U	0.47	Hengshui	T	V	RH	0.28
Luoyang	BLH	RH	V	0.16	Tangshan	U	V	RH	0.20
Zaozhuang	RH	T	U	0.46	Jinan	V	BLH	RH	0.59
Lianyungang	RH	V850	U	0.37	Qingdao	V	BLH	RH	0.26
Shangqiu	RH	T	V	0.48	Zibo	V	BLH	RH	0.59
Xuzhou	RH	BLH	V	0.48	Dongying	U	V	V850	0.36
Xuchang	BLH	RH	U	0.53	Yantai	V	BLH	U	0.33
Suqian	RH	T	MSLP	0.40	Weifang	BLH	T	U	0.34
Huaibei	RH	U	BLH	0.59	Weihai	RH	U	MSLP	0.36
Pingdingshan	BLH	RH	U	0.57	Dezhou	RH	V	BLH	0.40
Bozhou	RH	V	T	0.49	Liaocheng	BLH	V	RH	0.48
Zhoukou	RH	U	T	0.49	Binzhou	BLH	T	V	0.23
Luohe	RH	U	MSLP	0.45	Shaoxing	RH	BLH	T	0.59
Suzhou	RH	U	BLH	0.50	Jinhua	RH	TP	V	0.60
Huaian	RH	V	TP	0.42	Taizhou	V	RH	U	0.54
Yancheng	V	RH	BLH	0.37	Ningbo	RH	V	TP	0.48

Nanyang	RH	U	BLH	0.67	Wuhan	RH	V	BLH	0.61
Zhumadian	RH	TP	BLH	0.52	Changsha	RH	V	BLH	0.71
Fuyang	RH	V	U	0.64	Jingzhou	RH	V	BLH	0.55
Bengbu	RH	BLH	U	0.36	Yueyang	RH	BLH	V	0.60
Huainan	RH	BLH	U	0.56	Zhuzhou	RH	V	BLH	0.73
Xinyang	RH	TP	T	0.63	Xiangtan	RH	V	BLH	0.72
Suizhou	RH	BLH	U	0.63	Yichang	RH	U	V850	0.64
Shanghai	RH	V	TP	0.55	Yiyang	RH	V	BLH	0.67
Nanjing	V	RH	T	0.40	Changde	V	BLH	RH	0.59
Wuxi	RH	V	BLH	0.57	Jingmen	V	RH	U	0.63
Changzhou	V	RH	TP	0.49	Huangshi	RH	U	V850	0.72
Suzhou	RH	V	T	0.52	Huanggang	RH	U	V850	0.77
Nantong	V	RH	U	0.62	Xianning	RH	U	MSLP	0.74
Yangzhou	V	RH	T	0.52	Xiaogan	RH	V850	BLH	0.68
Zhenjiang	V	RH	T	0.55	Quzhou	V	RH	U	0.68
Taizhou	V	RH	T	0.59	Lishui	RH	V	T	0.70
Luan	RH	V	T	0.24	Wenzhou	RH	V	U	0.63
Hangzhou	RH	V	BLH	0.53	Jiujiang	V	RH	MSLP	0.58
Jiaxing	RH	V	T	0.45	Nanchang	V	RH	V850	0.67
Huzhou	V	RH	U	0.61	Jingdezhen	BLH	V850	T	0.59
Hefei	RH	TP	V	0.37	Shangrao	V850	BLH	RH	0.65
Wuhu	V	TP	U	0.46	Yingtai	BLH	V850	RH	0.64
Maanshan	V	U	TP	0.45	Yichun	V850	U	T	0.63
Tonglin	V	T	TP	0.50	Fuzhou	RH	V	BLH	0.72
Anqing	V	T	TP	0.56	Jian	BLH	U	RH	0.57
Chuzhou	RH	V	BLH	0.44	Xinyu	BLH	V	U	0.62
Chizhou	RH	V	BLH	0.47	Pingxiang	V850	BLH	T	0.61
Xuancheng	T	RH	U	0.27	-	-	-	-	-

**Table R2.** Meteorological drivers of 98% O<sub>3</sub> percentile and Pearson correlation coefficient between observed and modeled 98% O<sub>3</sub> percentile in each city of eastern China during May–September 2017–2022

	Meteorological variable					Meteorological variable			
	1 <sup>st</sup>	2 <sup>st</sup>	3 <sup>st</sup>	R		1 <sup>st</sup>	2 <sup>st</sup>	3 <sup>st</sup>	R
Taian	T	TP	TCC	0.71	Beijing	MSLP	BLH	V	0.30
Puyang	T	V850	TP	0.79	Tianjing	V	MSLP	BLH	0.27
Rizhao	T	U	TCC	0.67	Baoding	MSLP	V	BLH	0.28
Jining	T	TP	V850	0.77	Lanfang	MSLP	BLH	V	0.32
Xinxiang	T	TCC	BLH	0.74	Shijiazhuang	MSLP	BLH	V	0.24
Jiaozuo	T	TP	TCC	0.81	Handan	T	MSLP	U	0.31
Heze	T	V850	TP	0.78	Qinghuangdao	TCC	U	MSLP	0.36
Linyi	T	TP	TCC	0.73	Cangzhou	V	BLH	MSLP	0.35
Kaifeng	T	V850	TP	0.78	Xingtai	MSLP	BLH	V	0.25
Zhengzhou	T	V850	TP	0.78	Hengshui	V	MSLP	BLH	0.38
Luoyang	U	TCC	V	0.28	Tangshan	TCC	MSLP	T	0.27
Zaozhuang	T	TP	TCC	0.81	Jinan	T	TP	V850	0.77
Lianyungang	TCC	U	TP	0.68	Qingdao	U	BLH	RH	0.45
Shangqiu	T	TP	V850	0.71	Zibo	T	TP	V850	0.70
Xuzhou	T	TCC	TP	0.74	Dongying	T	RH	V	0.66
Xuchang	T	V850	TCC	0.70	Yantai	U	T	RH	0.44
Suqian	RH	TCC	TP	0.74	Weifang	T	TP	U	0.68
Huaipei	TCC	T	TP	0.74	Weihai	U	T	RH	0.44
Pingdingshan	T	V850	U	0.66	Dezhou	T	TP	V850	0.75
Bozhou	TCC	T	TP	0.67	Liaocheng	T	V850	TP	0.77
Zhoukou	T	TCC	RH	0.73	Binzhou	T	TP	V	0.66
Luohe	T	V850	RH	0.75	Shaoxing	T	V	TP	0.66

Suzhou	TCC	T	TP	0.71	Jinhua	T	V	TP	0.59
Huaian	T	TCC	TP	0.72	Taizhou	U	V	T	0.62
Yancheng	TP	V850	U	0.56	Ningbo	T	V	U	0.69
Nanyang	T	TCC	RH	0.74	Wuhan	TCC	RH	V850	0.75
Zhumadian	TCC	BLH	TP	0.67	Changsha	RH	TCC	V	0.76
Fuyang	RH	TCC	MSLP	0.74	Jingzhou	RH	V850	T	0.84
Bengbu	T	TCC	TP	0.72	Yueyang	RH	TCC	U	0.82
Huainan	TCC	RH	MSLP	0.68	Zhuzhou	RH	V	T	0.73
Xinyang	RH	TCC	U	0.74	Xiangtan	RH	V	TCC	0.78
Suizhou	RH	TCC	MSLP	0.75	Yichang	RH	TCC	V850	0.79
Shanghai	T	U	RH	0.72	Yiyang	RH	TCC	V850	0.80
Nanjing	TCC	V850	V	0.61	Changde	TCC	V850	T	0.74
Wuxi	TP	TCC	U	0.66	Jingmen	RH	V850	T	0.76
Changzhou	TCC	TP	BLH	0.60	Huangshi	RH	TCC	V	0.76
Suzhou	T	TP	U	0.63	Huanggang	TCC	RH	U	0.72
Nantong	T	RH	BLH	0.75	Xianning	RH	V850	T	0.80
Yangzhou	TCC	TP	V850	0.61	Xiaogan	RH	TCC	U	0.72
Zhenjiang	TCC	TP	MSLP	0.61	Quzhou	RH	V850	T	0.74
Taizhou	TCC	V850	U	0.61	Lishui	RH	U	V	0.65
Luan	TCC	MSLP	T	0.61	Wenzhou	U	RH	V	0.65
Hangzhou	TP	TCC	T	0.69	Jiujiang	TCC	V850	RH	0.80
Jiaxing	T	TP	U	0.70	Nanchang	RH	V850	T	0.72
Huzhou	TP	TCC	T	0.67	Jingdezhen	RH	V850	TCC	0.75
Hefei	TCC	TP	V	0.59	Shangrao	TCC	V850	T	0.76
Wuhu	TCC	TP	V	0.65	Yingtian	TCC	V850	T	0.78
Maanshan	TCC	TP	MSLP	0.66	Yichun	V850	TCC	T	0.75
Tonglin	TCC	MSLP	V	0.63	Fuzhou	V850	T	TCC	0.82
Anqing	TCC	V	TP	0.58	Jian	TCC	T	V	0.66
Chuzhou	TCC	TP	MSLP	0.58	Xinyu	V850	TCC	V	0.75
Chizhou	TCC	V	MSLP	0.63	Pingxiang	V850	TCC	V	0.75
Xuancheng	TCC	V	MSLP	0.58	-	-	-	-	-

**Point 3:** The authors conclude that the continuous NO<sub>x</sub> reduction during 2017–2022 is the reason for the differences in tendencies in the O<sub>3</sub> 98<sup>th</sup> and 2<sup>nd</sup> percentile trends. However, if you look carefully at Figure 5, which presents the anthropogenic impact for each year on the 98<sup>th</sup> and 2<sup>nd</sup> percentile trends, respectively, you will find that the anthropogenic impact shows a similar pattern for both trends until mid–2021. It appears that something that occurred after 2021 is the main reason for the divergence. More investigation is clearly needed. Also, how is this opposing trend sensitive to the period studied?

**Response 3:** Thanks for your constructive comments! We have corrected the problem in the MLR model according to Point 2, and the updated results is shown in Fig.R2. The trends for the monthly mean observed, meteorological, and anthropogenic 98<sup>th</sup> O<sub>3</sub> percentiles concentrations during May–September 2017–2021 are -0.363 ppb/year, -0.119 ppb/year (-33%), and -0.244 ppb/year (-67%), respectively (Table R3), and the trends for the monthly mean observed, meteorological, and anthropogenic 2<sup>nd</sup> O<sub>3</sub> percentiles concentrations are 0.027 ppb/year, -0.044 ppb/year (-163%), 0.071 ppb/year (263%), respectively. However, the trends

of monthly mean observed, meteorological and anthropogenic of 98<sup>th</sup> O<sub>3</sub> percentiles during May–September 2017–2022 are -0.178 ppb/year, 0.005 ppb/year (3%) and -0.183 ppb/year (-103%), respectively, and the trends of the observed, meteorological and anthropogenic of 2<sup>nd</sup> O<sub>3</sub> percentiles during May–September 2017–2022 are 0.115 ppb/year, 0.008 ppb/year (7%) and 0.107 ppb/year (93%), respectively.

Although anthropogenic emissions dominated variations in O<sub>3</sub> trends (May–September 2017–2022 and May–September 2017–2021), meteorological effects on O<sub>3</sub> trends cannot be ignored, particularly in 2022. Shadowed by mid–latitude atmospheric circulation, tropical sea–air coupling, and local land–air feedback processes, a record–breaking super–heatwave event occurred in most cities in eastern China in the summer of 2022, and some cities broke their highest temperature records (Zhang et al., 2023; Zhang et al., 2022). The most important meteorological variables in the MLR model were daily maximum temperature and RH (Tables R1 and R2). The temperature in eastern China showed that the monthly mean nighttime (daytime) temperature in June–August 2022 was 1.0 °C (1.1 °C), 0.8 °C (1.4 °C) and 2.2 °C (2.8 °C) higher than the monthly mean nighttime (daytime) temperature in June–August 2021, respectively (Fig. R3). The monthly mean nighttime (daytime) RH in eastern China in 2022 was 3.2% (3.1%), 1.9% (4.5%), and 9.4% (11%) lower than the monthly mean nighttime (daytime) RH in June–August 2021, respectively. Li et al. (2024) revealed that a sustained heatwave of extremely hot and dry summers in 2022 accelerate photochemical O<sub>3</sub> production by increasing anthropogenic and biogenic emissions and exacerbate O<sub>3</sub> accumulation by inhibiting dry deposition due to water–starved vegetation, resulting in an increase in O<sub>3</sub> pollution by more than 30% in urban areas. Our results also showed an increase in the meteorological components in the 98<sup>th</sup> and 2<sup>nd</sup> O<sub>3</sub> percentiles in 2022 relative to the meteorological components in the 98<sup>th</sup> and 2<sup>nd</sup> O<sub>3</sub> percentiles in 2021 (Fig.R2). Therefore, extremely hot and dry weather in 2022 will increase the peak and low O<sub>3</sub> concentrations in eastern China, which is probably the main reason for the difference between the May and September 2017–2021 and May–September 2017–2022 meteorological component trends. The above discussion was added to the manuscript, please refer to Page 13 Line 28–32 and Page 14 Line 1–19 in the manuscript.

In addition, the high relative humidity in 2020 and 2021, as well as the impact of COVID–19 pandemic also had a significant impact on the peak and low O<sub>3</sub> trend, which is analyzed in detail in **Point 4**.

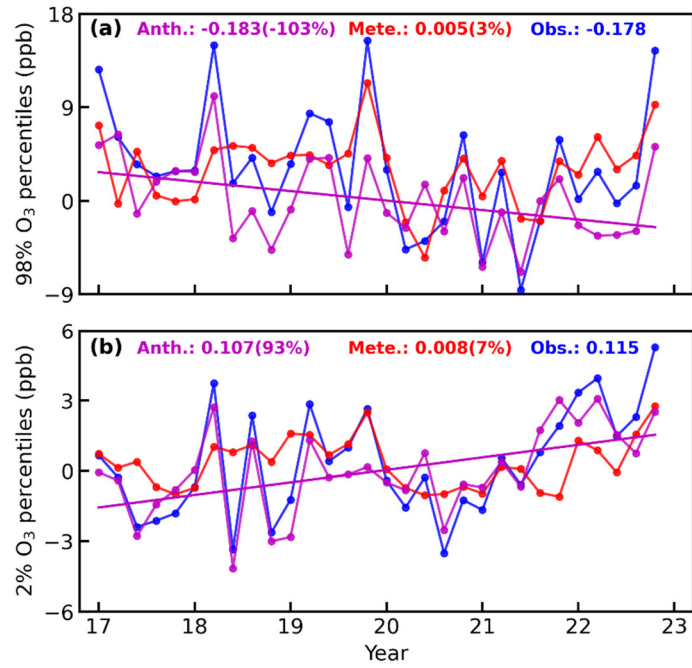


**Fig.R2** Trends of observed (blue lines), meteorological (red lines), and anthropogenic (red lines) (a) 98<sup>th</sup> and (b) 2<sup>nd</sup> O<sub>3</sub> percentiles component in eastern China during May–September 2017–2022. The labels at the top of each panel represent the trend in observed, meteorological, and anthropogenic components.

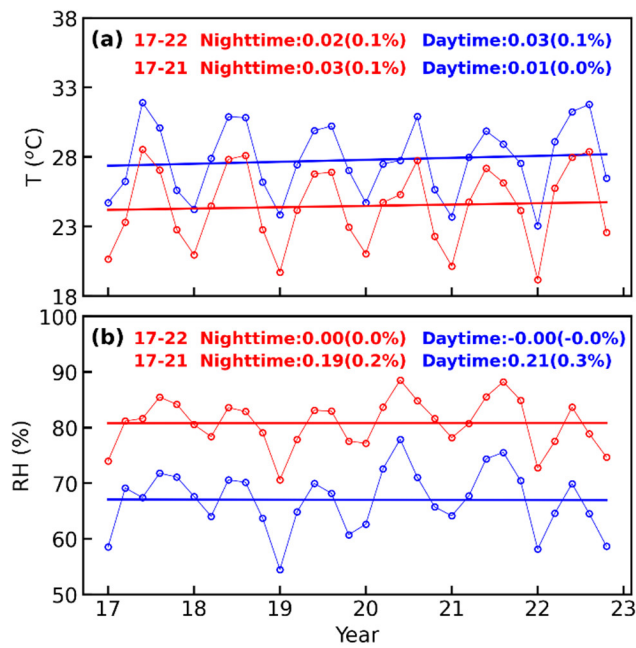


**Fig.R3** Trends of observed (a) 98<sup>th</sup> and (b) 2<sup>nd</sup> O<sub>3</sub> percentiles (blue lines), meteorological (a) 98<sup>th</sup> and (b) 2<sup>nd</sup> O<sub>3</sub> percentiles component (red lines) in MLR simulations, and the anthropogenic (a) 98<sup>th</sup> and (b) 2<sup>nd</sup> O<sub>3</sub> percentiles component (magenta lines) in eastern China during May–September 2017–2022. The labels at the top of each panel represent the trend in observed, meteorological, and anthropogenic components.

**Table R3.** Observed, Meteorologically, and anthropogenically driven trends of 2% and 98% O<sub>3</sub> percentiles in eastern China from 2017 to 2022 and from 2017 to 2021.

	May–September 2017–2022 trends						May–September 2017–2021 trends					
	2%			98%			2%			98%		
	Obs.	Mete.	Anth.	Obs.	Mete.	Anth.	Obs.	Mete.	Anth.	Obs.	Mete.	Anth.
Total	0.115	0.008	0.107	-0.178	0.005	-0.183	0.027	-0.044	0.071	-0.363	-0.119	-0.244
May	0.322	0.017	0.305	-0.020	-0.661	0.641	-0.438	-0.257	-0.181	-3.702	-0.968	-2.734
June	0.205	-0.032	0.237	-4.437	-1.894	-2.543	-0.364	-0.169	-0.195	-2.645	0.124	-2.769
July	0.768	-0.177	0.945	-1.745	-1.100	-0.645	0.665	-0.247	0.912	-2.974	-2.370	-0.604
August	0.371	0.084	0.287	-0.687	-0.156	-0.531	-0.003	-0.260	0.257	-1.473	-0.908	-0.565
September	1.290	0.319	0.971	1.999	1.136	0.863	0.884	-0.126	1.010	1.352	0.814	0.538

**Point 4:** The authors have not directly answered why the 2<sup>nd</sup> percentile O<sub>3</sub> increased over 2017–2022. The 2<sup>nd</sup> percentile should be related to nighttime O<sub>3</sub>, while the entire manuscript discusses the O<sub>3</sub> photochemical formation regime, which is a daytime indicator. More investigation is needed on the nighttime process, such as NO titration of O<sub>3</sub>, loss of O<sub>3</sub> with VOCs, etc.

**Response 4:** We agree with this suggestion. Because vertical profiles of O<sub>3</sub> precursors at night are not available due to MAX–DOAS observational limitations, we discuss the possible increase in 2<sup>nd</sup> O<sub>3</sub> percentile based on surface observations and MLR modelling results. It has been analysed in **Point 3** that the extreme hot and dry in 2022 increases the 98<sup>th</sup> and 2<sup>nd</sup> O<sub>3</sub> percentile concentrations, which is mainly a meteorological effect.

If we look carefully at Fig.R2, which presents the anthropogenic impact for each year on the 98<sup>th</sup> and 2<sup>nd</sup> percentile trends, respectively, we will find that the observed increase in 2<sup>nd</sup> O<sub>3</sub> percentile was mainly concentrated after 2020, up to 0.44 ppb/year. The meteorological components did not change significantly in 2020 and 2021 but considerably increased in 2022, with a trend of 0.17 ppb/year 2020–2022. This rapid increase in 2<sup>nd</sup> O<sub>3</sub> percentile is mainly caused by anthropogenic emissions, with a trend of 0.27 ppb/year 2020–2022. Owing to the impact of the COVID–19 pandemic, the decrease in NO<sub>x</sub> concentrations was most significant in 2020–2022 (Fig.3b), and the substantial reduction in NO<sub>x</sub> concentrations weakened the O<sub>3</sub> titration of NO, resulting in an increase in nighttime O<sub>3</sub> concentrations, which was also confirmed by the significant negative correlation between the trend of the 98<sup>th</sup> NO<sub>2</sub> percentile and the trend of the 2<sup>nd</sup> O<sub>3</sub> percentiles during May–September 2017–2022 (Fig.4b). A recent study showed that nighttime O<sub>3</sub> depletion in China is mainly caused by the wet–scavenging effect and O<sub>3</sub> titration from fresh NO emissions (Li et al., 2023). The wet–scavenging effect

was similar to the effect of precipitation, the higher the ambient humidity, the more conducive it was to O<sub>3</sub> depletion. The RH at night increased slowly in eastern China during May–September of 2017–2021 (Fig.R3b), and the nighttime RH in 2020 and 2021 was higher than that in other years. Moreover, a general wetting trend has been detected in eastern China during the summer in recent years (Hu et al., 2021). RH had the most significant effect on 2<sup>nd</sup> O<sub>3</sub> percentile trends according to MLR results (Table R1). Therefore, the meteorological component had an inhibitory effect on the increase in the 2<sup>nd</sup> O<sub>3</sub> percentile trends during May–September 2017–2021. However, owing to the significant emission reduction of NO<sub>x</sub> concentrations, the titration of NO<sub>x</sub> was weakened, and the decrease in O<sub>3</sub> depletion at night led to an increase in the overall 2<sup>nd</sup> O<sub>3</sub> percentile trends.

In conclusion, owing to the impact of the COVID–19 pandemic (significant decrease in NO<sub>x</sub> concentrations) and unfavorable meteorological conditions (high relative humidity) in 2020 and 2021 in eastern China, the 98<sup>th</sup> O<sub>3</sub> percentile concentration in 2020 and 2021 was lower (compared to the 98<sup>th</sup> O<sub>3</sub> percentile concentration in 2018 and 2019), while the 2<sup>nd</sup> O<sub>3</sub> percentile concentration showed a rapid upward trend. In addition, the extremely hot and dry meteorological conditions in 2022 will increase the 98<sup>th</sup> and 2<sup>nd</sup> O<sub>3</sub> percentile concentrations, weakening the decreasing trend in peak O<sub>3</sub> concentrations and increasing the upward trend at low O<sub>3</sub> concentrations. The above discussion was added to the manuscript, please refer to Page 14 Line 31–34 and Page 15 Line 1–18 in the manuscript.

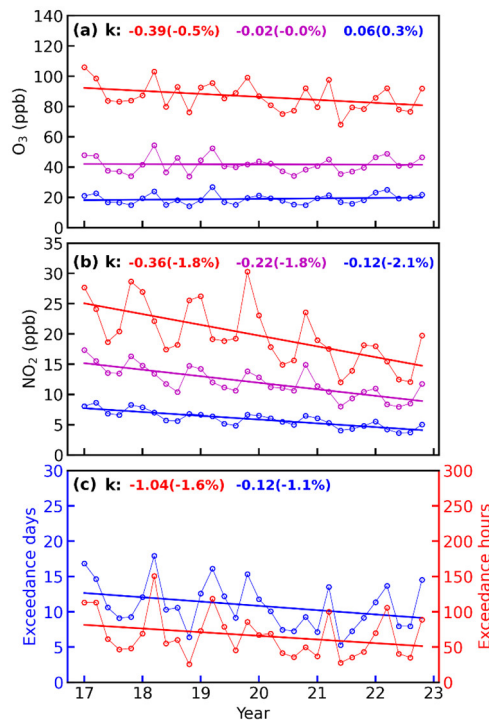


**Fig.R4.** Trends of surface (a) O<sub>3</sub>, (b) NO<sub>2</sub>, (c) O<sub>3</sub> exceedance days and O<sub>3</sub> exceedance hours in eastern China during May–September 2017–2022. The red, magenta, and blue solid lines in (a) and (b) indicate the trends for the 98<sup>th</sup>, 50<sup>th</sup>, and 2<sup>nd</sup> percentiles, respectively. The labels on (a) and (b) represent the trends in O<sub>3</sub> and NO<sub>2</sub> for May–September 2017–2022, units: ppb/year. The labels on (c) represent the trends in O<sub>3</sub> exceedance days and O<sub>3</sub> exceedance hours for May–September 2017–2022. The percentage change is indicated in brackets.

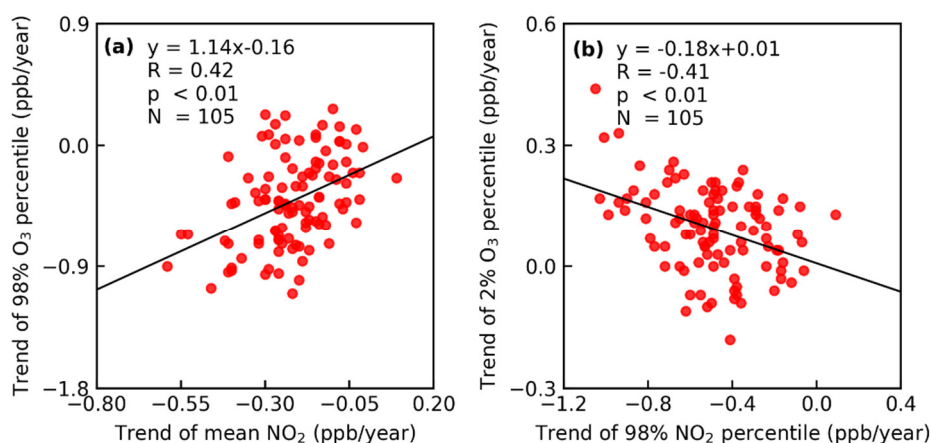


**Fig.R5.** Scatterplots showing the relationships between the (a) trend of mean NO<sub>2</sub> concentrations and the trend of 98<sup>th</sup> O<sub>3</sub> percentiles, (b) trend of 98<sup>th</sup> NO<sub>2</sub> percentiles and trend of 2<sup>nd</sup> O<sub>3</sub> percentiles in each city of eastern China during May–September 2017–2022. The correlation coefficients are shown in the top left of each panel, N=number of cities.

**Point 5:** In Section 3.4, although this section should be removed according to my comment #1, conflicts between Figure 9 and Figure S9 are noted. The area proportions presented in Figure 9 are not consistent with the spatial patterns in Figure S9. For example, Figure 9d suggests a NO<sub>x</sub>-limited region up to 75% of the total MLYRP in August of 2022, while Figure S9 shows a NO<sub>x</sub>-limited area smaller than the VOC-limited area. Please check your analysis.

**Response 5:** Thanks for pointing out the conflicts among the figures! We carefully examined the reasons for the conflicting images, which were mainly attributed to differences in data processing. Fig.R6 is based on daily FNR to determine the area proportion of the VOC-limited regime, Transition regime, and NO<sub>x</sub>-limited regime areas, while Fig.R7 is based on monthly mean FNR to determine the area proportion of the VOC-limited regime, Transition regime, and NO<sub>x</sub>-limited regime areas. Fig.R6 shows the trends of TROPOMI observed area proportion for VOC-limited regime, Transition regime, and NO<sub>x</sub>-limited regime over Huaihe river basin during May–September 2018–2022. Here we first determined the O<sub>3</sub> formation

sensitivity based on the daily FNR observed by TROPOMI (FNR <2.1 for VOC–limited regime, FNR>3.2 for NO<sub>x</sub>–limited regime), and then calculated the area proportion of the daily VOC–limited regime, Transition regime, and NO<sub>x</sub>–limited regime areas. Finally, the monthly average of the area proportion of daily VOC–limited regime, Transition regime, and NO<sub>x</sub>–limited regime areas was taken and the trend was calculated, as shown in Fig.R6, the light red dots in (b–d) represent the daily values, and the solid red dots are monthly mean values. Fig.R7 shows the spatial and temporal variations of monthly mean FNR from May–September 2018–2022. the monthly mean FNR was calculated firstly based on TROPOMI observed daily FNR, then threshold value 2.1 and 3.2 was used for monthly mean FNR to determine the O<sub>3</sub> formation sensitivity. This section was removed according to **Point 1**.

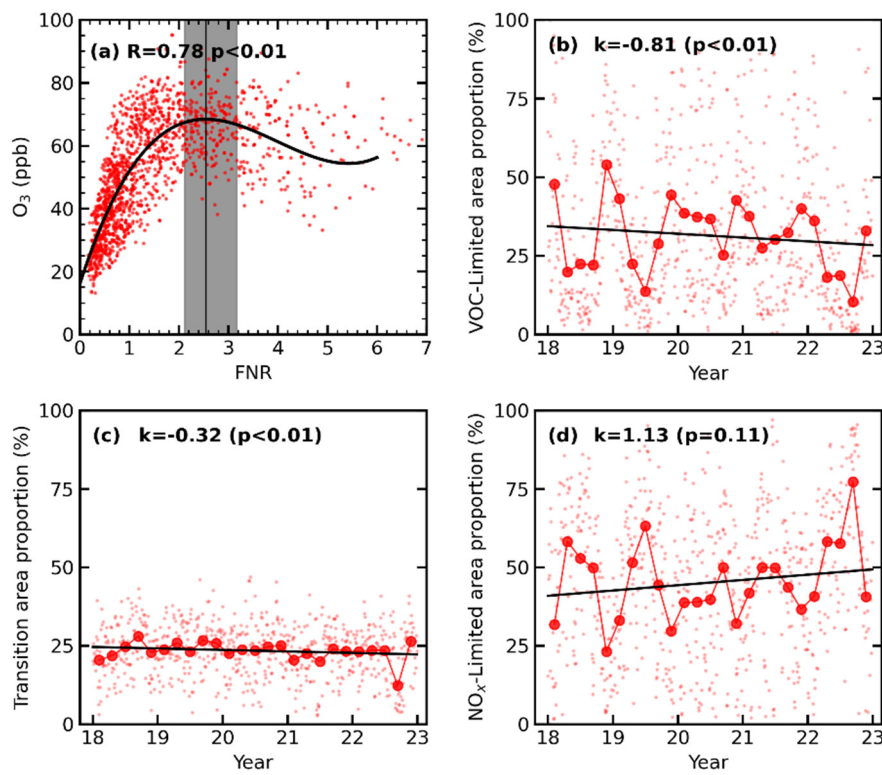


**Fig.R6.** (a) Variation of monthly mean O<sub>3</sub> (~13:30) with monthly mean TROPOMI FNR in HRB during May–September 2022. The solid line represents third–order polynomial fitting. The vertical line represents the maximum value of the fitted curve, and the vertical shadow represents the range of the curve slope from –3 to +3 (transition regime). Trends of TROPOMI observed area proportion for (b) VOC–limited regime, (c) Transition regime, and (c) NO<sub>x</sub>–limited regime over HRB during May–September 2018–2022. The light red dots in (b–d) represent the daily values, and the solid red dots are monthly mean values.

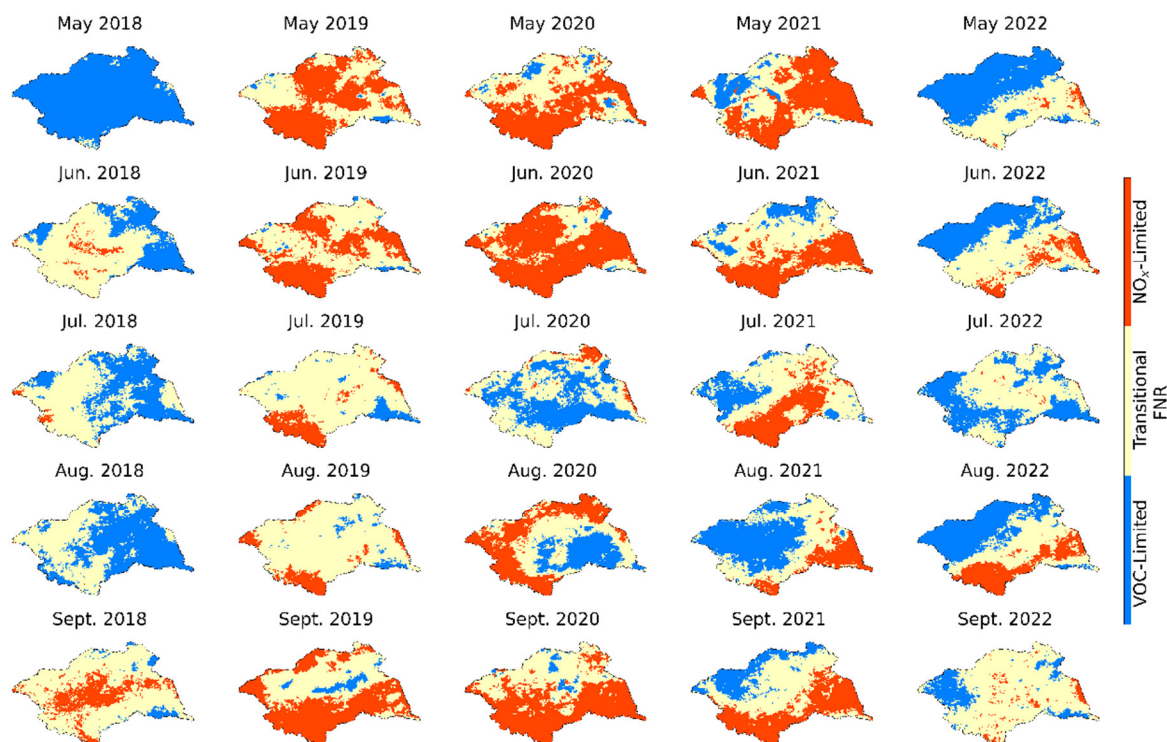


**Fig.R7.** Spatial and temporal variations of monthly mean FNR from May–September 2018–2022. The date is shown at the top of each panel.

**Specific comments:**

1. Section 2.3, could the authors elaborate more on how trustworthy is the TROPOMI O<sub>3</sub> profile retrieval?

Based on **Point 1**, we have deleted section 3.4 (Interannual differences in surface O<sub>3</sub> formation sensitivity), and the O<sub>3</sub> profile observed by TROPOMI was not employed in the manuscript. Thus, we also removed the description of the TROPOMI O<sub>3</sub> profile retrieval in the manuscript.

2. Lines 20–22, Page 8, could the authors say more about why 5<sup>th</sup>, 50<sup>th</sup>, and 95<sup>th</sup> could represent background, typical, and polluted conditions.

Different percentiles may be related to different influences, such as background concentration levels, emission changes, climate change, and regional transport effects (Lefohn et al., 2010). In principle, the lowest daily O<sub>3</sub> concentrations usually occur before sunrise due to nighttime titration of NO, and the low percentile (2<sup>nd</sup>) usually characterizes baseline or background conditions because increases in the low O<sub>3</sub> percentile tend to be associated with increases in baseline or background O<sub>3</sub> concentrations. Similar conclusions were also obtained from both models and observations (Jacob et al., 1999; Cynthia Lin et al., 2000). O<sub>3</sub> pollution

in eastern China generally occurs in the late afternoon on clear days in the warm season (Wang et al., 2022), when the ambient O<sub>3</sub> concentration is highest, so the high percentile (98<sup>th</sup>) characterizes the conditions of the pollution events. The middle percentiles (25<sup>th</sup>, 50<sup>th</sup> and 75<sup>th</sup>) usually follow the same trend as the mean values and therefore represent typical conditions (Cooper et al., 2012; Li et al., 2022). We have added this statement to the manuscript, please refer to Page 8 Line 6–17 in the manuscript.

3. Lines 5–6, Page 12: Why is the primary HCHO contribution much higher than the secondary HCHO at these sites, differing from previous findings cited in the paper? Please provide some explanation.

Atmospheric primary HCHO concentrations are mainly derived from motor vehicle exhaust, petrochemical industry, solvent use, and combustion emissions (Ma et al., 2019). Hefei, Huaibei, and Tai'an are located in the NCP, which is the region with the highest primary emissions of air pollutants in China (Li et al., 2017). The rapid industrialization and urbanization in these developing cities has influenced the primary and secondary HCHO concentrations, and HCHO mainly stems from initial atmospheric pollutants (Lu et al., 2024). Although the articles cited in our manuscript show that secondary HCHO concentrations are much higher than that of primary HCHO, the primary HCHO has also been found to be much higher than secondary HCHO in other cities in China, such as Shenyang (Ma et al., 2019), Lanzhou (Lu et al., 2024), Chengdu (Bao et al., 2022), Nanjing (Hong et al., 2018). Primary HCHO concentrations in Hefei, Huaibei and Tai'an usually reach their maximum in the morning and evening, and vehicle emissions may be the main source of primary HCHO, as industrial emissions do not show a significant diurnal pattern (Hong et al., 2018). We have added this statement to the manuscript, please refer to Page 12 Line 9–14 in the manuscript.

#### **Technical corrections:**

1. Replace “unbalanced emission reduction in ozone precursors” with NO<sub>x</sub> reduction throughout the text?

We have followed this suggestion and carefully checked the manuscript for similar expressions.

2. Line 28, Page 1, remove “experiment”.

Thanks for pointing out the unsuitable expression. We have followed this suggestion and corrected the mistake accordingly.

3. Line 25, Page 2, Zhai et al. (2019) is a PM<sub>2.5</sub> study, not ozone study. Please remove. Also in Line 3, Page 4.

Thanks for pointing out the inappropriate quote, we have corrected the relevant mistakes and carefully checked the manuscript for similar errors.

4. Line 5, Page 3, it should be Li et al. (2020a).

Thanks for pointing out the unsuitable expression, we have corrected the relevant mistakes.

5. Line 22, Page 3, it should be “diagnose”.

Thanks for pointing out the unsuitable expression, we have corrected the relevant mistakes.

6. Line 24, Page 8, do not use “one-sided understanding”.

We have followed this suggestion and carefully checked the manuscript for similar expressions.

7. In Figure 5, the authors seem to fit the observed monthly O<sub>3</sub> and use the fitted lines to connect monthly values. Please replace these with straight lines directly connecting the dots.

Thanks for your suggestion. We have followed this suggestion and replotted the figure. Please refer to Fig.6 in the manuscript.

8. References, journal names should be included.

Thanks for your suggestion. We have followed this suggestion and reorganized the format of the references.

#### Reference:

Bao, J., Li, H., Wu, Z., Zhang, X., Zhang, H., Li, Y., Qian, J., Chen, J., and Deng, L.: Atmospheric carbonyls in a heavy ozone pollution episode at a metropolis in Southwest China: Characteristics, health risk assessment, sources analysis, *J. Environ. Sci-China*, 113, 40-54, 10.1016/j.jes.2021.05.029, 2022.

Cooper, O. R., Gao, R. S., Tarasick, D., Leblanc, T., and Sweeney, C.: Long-term ozone trends at rural ozone monitoring sites across the United States, 1990–2010, *J. Geophys. Res-atmos.*, 117, 10.1029/2012jd018261, 2012.

Cynthia Lin, C. Y., Jacob, D. J., Munger, J. W., and Fiore, A. M.: Increasing background ozone in surface air over the United States, *Geophys. Res. Lett.*, 27, 3465-3468, 2000.

Hong, Q., Liu, C., Chan, K. L., Hu, Q., Xie, Z., Liu, H., Si, F., and Liu, J.: Ship-based MAX-DOAS measurements of tropospheric NO<sub>2</sub>, SO<sub>2</sub>, and HCHO distribution along the Yangtze River, *Atmos. Chem. Phys.*, 18, 5931-5951, 10.5194/acp-18-5931-2018, 2018.

Hu, W., She, D., Xia, J., He, B., and Hu, C.: Dominant patterns of dryness/wetness variability in the Huang-Huai-Hai River Basin and its relationship with multiscale climate oscillations, *Atmos. Res.*, 247, 105148, 2021.

Jacob, D. J., Logan, J. A., and Murti, P. P.: Effect of rising Asian emissions on surface ozone in the United States, *Geophys. Res. Lett.*, 26, 2175-2178, 1999.

Lefohn, A. S., Hazucha, M. J., Shadwick, D., and Adams, W. C.: An alternative form and level of the human health ozone standard, *Inhal. Toxicol.*, 22, 999-1011, 2010.

Li, K., Jacob, D. J., Liao, H., Shen, L., Zhang, Q., and Bates, K. H.: Anthropogenic drivers of 2013–2017 trends in summer surface ozone in China, *Proc. Natl. Acad. Sci.*, 116, 422-427, 10.1073/pnas.1812168116, 2018.

Li, K., Jacob, D. J., Shen, L., Lu, X., De Smedt, I., and Liao, H.: Increases in surface ozone pollution in China from 2013 to 2019: anthropogenic and meteorological influences, *Atmos. Chem. Phys.*, 20, 11423-11433, 10.5194/acp-20-11423-2020, 2020.

Li, M., Huang, X., Yan, D., Lai, S., Zhang, Z., Zhu, L., Lu, Y., Jiang, X., Wang, N., Wang, T., Song, Y., and Ding, A.: Coping with the concurrent heatwaves and ozone extremes in China under a warming climate, *Sci. Bull.*, 10.1016/j.scib.2024.05.034, 2024.

- Li, M., Liu, H., Geng, G., Hong, C., Liu, F., Song, Y., Tong, D., Zheng, B., Cui, H., Man, H., Zhang, Q., and He, K.: Anthropogenic emission inventories in China: a review, *Natl. Sci. Rev.*, 4, 834-866, 10.1093/nsr/nwx150, 2017.
- Li, X.-B., Yuan, B., Parrish, D. D., Chen, D., Song, Y., Yang, S., Liu, Z., and Shao, M.: Long-term trend of ozone in southern China reveals future mitigation strategy for air pollution, *Atmos. Environ.*, 269, 10.1016/j.atmosenv.2021.118869, 2022.
- Li, X., Ren, J., Huang, R., Chen, L., Li, Y., Qiao, X., Cheng, Y., Zhao, B., Yin, D., Gao, D., Sun, Y., and Zhang, F.: The Aggravation of Summertime Nocturnal Ozone Pollution in China and Its Potential Impact on the Trend of Nitrate Aerosols, *Geophys. Res. Lett.*, 50, 10.1029/2023gl103242, 2023.
- Liu, Y., Geng, G., Cheng, J., Liu, Y., Xiao, Q., Liu, L., Shi, Q., Tong, D., He, K., and Zhang, Q.: Drivers of Increasing Ozone during the Two Phases of Clean Air Actions in China 2013–2020, *Environ. Sci. Technol.*, 57, 8954-8964, 10.1021/acs.est.3c00054, 2023.
- Lu, C., Li, Q., Xing, C., Hu, Q., Tan, W., Lin, J., Zhang, Z., Tang, Z., Cheng, J., Chen, A., and Liu, C.: Identification of O<sub>3</sub> Sensitivity to Secondary HCHO and NO<sub>2</sub> Measured by MAX-DOAS in Four Cities in China, *Remote Sens.*, 16, 10.3390/rs16040662, 2024.
- Ma, Z., Liu, C., Zhang, C., Liu, P., Ye, C., Xue, C., Zhao, D., Sun, J., Du, Y., Chai, F., and Mu, Y.: The levels, sources and reactivity of volatile organic compounds in a typical urban area of Northeast China, *J. Environ. Sci-China*, 79, 121-134, 10.1016/j.jes.2018.11.015, 2019.
- Wang, W., Parrish, D. D., Wang, S., Bao, F., Ni, R., Li, X., Yang, S., Wang, H., Cheng, Y., and Su, H.: Long-term trend of ozone pollution in China during 2014–2020: distinct seasonal and spatial characteristics and ozone sensitivity, *Atmos. Chem. Phys.*, 22, 8935-8949, 10.5194/acp-22-8935-2022, 2022.
- Zhai, S., Jacob, D. J., Wang, X., Shen, L., Li, K., Zhang, Y., Gui, K., Zhao, T., and Liao, H.: Fine particulate matter (PM<sub>2.5</sub>) trends in China, 2013–2018: separating contributions from anthropogenic emissions and meteorology, *Atmos. Chem. Phys.*, 19, 11031-11041, 10.5194/acp-19-11031-2019, 2019.
- Zhang, T., Deng, Y., Chen, J., Yang, S., and Dai, Y.: An energetics tale of the 2022 mega-heatwave over central-eastern China, *Npj Clim. Atmos. Sci.*, 6, 10.1038/s41612-023-00490-4, 2023.
- Zhang, T., Tam, C.-Y., Lau, N.-C., Wang, J., Yang, S., Chen, J., Yu, W., Jiang, X., and Gao, P.: Influences of the boreal winter Arctic Oscillation on the peak-summer compound heat waves over the Yangtze–Huaihe River basin: the North Atlantic capacitor effect, *Clim. Dyn.*, 59, 2331-2343, 10.1007/s00382-022-06212-5, 2022.